Alexandria Engineering Journal 85 (2023) 132–145

Contents lists available at ScienceDirect

Alexandria Engineering Journal

journal homepage: www.elsevier.com/locate/aej

ORIGINAL ARTICLE

Two-strain mathematical virus model with delay for Covid-19 with immune response

Oumar Abdallah I. [a], Tchepmo Djomegni P.M. [b,c,*], Daoussa Haggar M.S. [a], Abdramana A.S. [a]

[a] Laboratoire de Modélisation, Mathématiques, Informatique, Applications et Simulation, Université de N'Djamena, P.O Box: 1027, Chad
[b] School of Mathematical and Statistical Science, North West University, 11 Hoffman Street, Potchefstroom 2351, South Africa
[c] DSI-NRF Centre of Excellence in Mathematical and Statistical Sciences (CoE-MaSS), South Africa

ARTICLE INFO

MSC:
92B05
37D05
34D20
34D23

Keywords:
Virus model
Hopf bifurcation
Delay differential equations
Optimal control
Basic reproduction number
Stability analysis
Sensitivity index

ABSTRACT

In this manuscript, we analyze a new virus model of SARS-CoV-2 infection with immune response. The initial model was proposed by Mochan et al. [23] to describe an experiment made on Macaques. We consider the latent period of newly infected cells by introducing a delay in the model. We fully analyze the quality properties of the model and investigate strategies to reduce secondary infections. Moreover, we investigate the impact of the latent period on the spread of the infection. We observe due to the delay, the possibility to reach an infection-free state when $\mathcal{R}_0 > 1$. This observation is not possible when the delay is not considered. We also demonstrate the occurrence of a Hopf bifurcation when $\mathcal{R}_0 > 1$. We further introduce two control parameters to prevent new infections and inhibit viral production, and we formulate an optimal control problem aiming to minimize infections, virus proliferation and the cost of treatment. We establish the existence of the optimal solution and illustrate the theoretical results numerically. In contrast to Mochan et al. [23] results, our simulations show that increased suppression of viral production can change a lethal or chronic infection to a survivable scenario or acute infection. We also observe that the latency period can cause several states of chronic infection before the host recovers totally. Moreover, the density of viruses increases as the latent period is long. The reason being that the immune system is alerted with a delay (after the latent period), which is an advantage for the replication of viruses.

1. Introduction

With more than 760 million cases and 6.8 million fatalities worldwide by April 2023, the novel coronavirus SARS-CoV-2 (severe acute respiratory syndrome coronavirus 2) has become the most serious global pandemic since the Spanish flu of 1918-1920. It was first discovered in Wuhan, China, at the end of 2019. SARS-CoV-2 can spread from person to person through direct contact with an infected host or through droplet infection. There have also been reports of transmission through the faecal-oral route and from asymptomatic carriers. To describe the epidemiological aspects of the transmission dynamics of the COVID-19 epidemic, a significant number of mathematical modeling studies have been conducted [35,30,32,16,6,36,2,8,10,21,25,28,31,33,3,4]. A few have attempted to describe the infection dynamics between the immune system and the virus. Coronaviruses often affect the upper respiratory tract and produce mild symptoms. However, the SARS-CoV-2 is a more complicated coronavirus that can proliferate in the lower respiratory tract and cause pneumonia, which can be fatal. The virus spreads through respiratory droplets, with a median incubation time of about 4-5 days [12,29,19,20] and a presymptomatic period of 6-9 days, with symptoms appearing in 97.5% of symptomatic patients within 11.5 days [19]. The most common signs of COVID-19 infection in patients are a fever and a dry cough. Previous research on SARS-CoV has shown that it mostly affects airway epithelial cells [31]. The virus destroys epithelial cells, inducing an immunological reaction. The first line of defense is the activation of macrophages in response to the injury; concurrently, the release of cytokines and chemokines that promote inflammation, such as IL-6 and IFN [13], attracts immune cells, particularly T- and B-cells, but more specifically helper T-lymphocytes of class 1 [14]. According to clinical evidence, these cytokine storms induce lung inflammation, which results in septic shock and multi-organ failure. Moreover, greater levels of interleukines demonstrate an immune response that is dysfunctional [13].

* Corresponding author.
E-mail address: ptchepmo@gmail.com (P.M. Tchepmo Djomegni).

https://doi.org/10.1016/j.aej.2023.11.020
Received 1 August 2023; Received in revised form 28 October 2023; Accepted 7 November 2023
Available online 19 November 2023

A mathematical model of immune viral dynamics for SARS-CoV-2 therapeutic development was put forth by Cao et al. [5]. According to their findings, it takes approximately 32.6 days to reach 50% of the maximum cell-based immunity. Wang et al. [34] investigated in their model how the SARS-CoV-2 virus interacts with cells and immune responses in order to understand the pathogenic aspects of the illness. Their simulation demonstrates that the duration of the viral plateau phase can be decreased and the time to recover can be slashed when anti-inflammatory or antiviral medications are taken in conjunction with interferon. Chatterjee et al. [7] developed a mathematical model of within-host SARS-CoV-2 infection that considers the key components of the innate immune and CD8 T-cell responses. Their model accurately captured the full range of outcomes achieved by adjusting the timings and intensities of the two immunological arms. Mochan et al. [23] proposed a new model that emphasizes the significance of the inflammatory response to viral infection, using information from pro-inflammatory mediators to combat viral growth. Moreover, it captures the motions in the lower and upper respiratory tracts. Although SARS-Cov-2 experimental data from rhesus macaque infection has been shown to be comparable to that in people [Josset et al. [18], Munster et al. [24]], they fitted their model to it. Unlike their approaches, we do not explicitly incorporate in this work the anti-inflammatory response and damage cellular. However, we consider the delay in the infection rate by assuming that newly infected cells first go through a latent period τ before being able to infect other cells. The reasons for considering delays are not only mathematically but biologically motivated. First, there is a time frame after a cell is infected to become infectious. For the case of HIV infection, the latency period is estimated between six hours and two days before the infected cells begin to infect others [22,26]. SARS-CoV enters the cell by direct fusion and has a latency period of 6 h [27]. SARS-CoV-2 has been shown to exhibit a two-step transcriptional strategy during the first 24 hours of infection, comprising a lag phase that ends when the virus pauses and a log phase that begins when the virus load increases rapidly. Interestingly, the host's innate immune response was found not to be activated (latency period) until the virus enters the log phase [17]. We fully analyze the delayed mathematical model and investigate the strategies to limit cell infection. We also assess the impact of the latency period on the overall dynamics of the infection.

2. Model analysis

We analyze a covid-19-induced inflammatory response model. The model describes the dynamics of the virus as seen in macaque experiments. The lower respiratory tract (LRT) is the first part of the body where the virus settles after which it might spread to the upper respiratory tract (URT). Healthy epithelial cells are the target of the virus. Infected cells stimulate the production of free viruses, which can then be eliminated by the internalization of epithelial cells, antibodies, or a generalized immunity. They cause the immune system's pro-inflammatory mechanism to become active. The presence of pro-inflammatory mediators hinders the creation of viruses by reducing the capacity of infected cells to produce virions. Anti-inflammatory mediators then rise in response to inflammation, limiting the production of more inflammatory mediators and defending the host against cytokine storms. In addition to the virus, pro-inflammatory mediators also significantly harm the body by killing epithelial cells [23]. Mochan et al. [23] formulated a new mathematical model to reflect this scenario and fitted the model to experimental data. Given the complexity of the equations due to their choice of the standard incidence functions, they only performed numerical simulations to investigate the effect of parameters on the overall dynamic. Unlike their approaches, we do not explicitly represent the classes of damaged cellular and anti-inflammatory mediators created in response to pro-inflammatory signals. However, we consider the latent period of newly infected cells by introducing a time-delay, and a mass action incidence. We study the qualitative properties of the model and investigate the impact of the delay on the spread of cell infection. We also propose a delay optimal control model aiming to minimize infections at optimal costs. The fundamental principle governing the model is the following:

- ▷ rate of change of virus (V) = virus production ± migration from LRT to URT - deaths.
- ▷ rate of change of healthy cells (H) = growth - infection - death due to inflammation.
- ▷ rate of change of infected cells (I) = new infections - death (natural or due to inflammation).
- ▷ rate of change of pro-inflammatory mediators (F) = production (proportional to density of infected cells) - degradation.

The resulting mathematical equations are

$$\frac{dV_U(t)}{dt} = \gamma_V I_U(t) - \gamma_{VH} V_U(t) H_U(t) - \alpha_{VH} V_U(t) - a_{VH} V_U(t) + \beta V_L(t) = f_1 \tag{2.1}$$

$$\frac{dH_U(t)}{dt} = b_{HD}(H_{max} - H_U(t) - I_U(t)) H_U(t) - \gamma_{HV} V_U(t) H_U(t) - a_{HF} F(t) H_U(t) = f_2 \tag{2.2}$$

$$\frac{dI_U(t)}{dt} = \gamma_{HV} V_U(t-\tau) H_U(t-\tau) - a_{IF} F(t) I_U(t) - a_I I_U(t) = f_3 \tag{2.3}$$

$$\frac{dV_L(t)}{dt} = \gamma_V I_L(t) - \gamma_{VH} V_L(t) H_L(t) - \alpha_{VH} V_L(t) - a_{VH} V_L(t) - \beta V_L(t) = f_4 \tag{2.4}$$

$$\frac{dH_L(t)}{dt} = b_{HD}(H_{max} - H_L(t) - I_L(t)) H_L(t) - \gamma_{HV} V_L(t) H_L(t) - a_{HF} F(t) H_L(t) = f_5 \tag{2.5}$$

$$\frac{dI_L(t)}{dt} = \gamma_{HV} V_L(t-\tau) H_L(t-\tau) - a_{IF} F(t) I_L(t) - a_I I_L(t) = f_6 \tag{2.6}$$

$$\frac{dF(t)}{dt} = b_{FI}(I_U(t) + I_L(t)) - a_F F(t) = f_7, \tag{2.7}$$

where V_U/V_L are the densities of virus present in the URT/LRT, H_U/H_L the densities of healthy epithelial cells in the URT/LRT, I_U/I_L the densities of infected epithelial cells present in the URT/LRT and F the density of pro-inflammatory mediator. The description of the parameters is given in Table 1. Endowed with the initial condition, the above model can be written in the compact form

$$x'(t) = f(x(t), x_\tau(t)), \quad t > 0 \tag{2.8}$$

$$x(r) = \phi(r), \quad r \in [-\tau, 0], \tag{2.9}$$

Table 1
Description of model parameters (2.1)-(2.7).

γ_V	virus replication rate
γ_{VH}	Absorption rate of virus by epithelial cells
α_{VH}	rate of upper respiratory virus destruction by adaptive immunity
a_{VH}	upper respiratory tract virus kill rate by non-specific immunity
β	virus migration rate from LRT to URT
b_{HD}	regeneration rate of healthy epithelial cells
a_{HF}	damage rate of healthy cells by inflammation
a_{IF}	damage rate of infected cells by inflammation
a_I	death rate of infected cells
γ_{HV}	rate of infection of healthy cells by the virus
H_{max}	maximum capacity of epithelial cells in each airway
b_{FI}	rate of stimulation of inflammation by the presence of infected cells
a_F	inflammation decay rate
γ_{FG}	rate of stimulation of anti-inflammatory signal by inflammation
a_G	rate of degradation of the anti-inflammatory mediator

where $x=(V_U,H_U,I_U,V_L,H_L,I_L,F)^T$, $x_\tau(t)=x(t-\tau)$, $f=(f_1,f_2,f_3,f_4,f_5,f_6,f_7)^T$ and $\phi:[-\tau,0]\to\mathbb{R}^7$ is a given function. Since f is a polynomial function (with variables x and x_τ), it is of class C^∞. Hence, the problem (2.8)-(2.9) has a unique solution defined on an interval $[-\tau,\sigma]$, with $\sigma>0$. For the rest of the analysis, we will assume that the solution is positive and bounded.

2.1. Equilibrium points

There are four disease free equilibrium points $E_0=(0,0,0,0,0,0,0)$, $E_1=(0,0,0,0,H_{max},0,0)$, $E_2=(0,H_{max},0,0,0,0,0)$ and $E_3=(0,H_{max},0,0,H_{max},0,0)$. The three endemic equilibrium points:

- Associated to URT: $E_4=(H_U^*,I_U^*,V_U^*,0,0,0,F^*)$, where $I_U^*=\frac{a_F b_{HD}H_{max}}{a_{HL}b_{FI}}$, $V^*=\frac{b_{FI}a_{HL}H_{max}(\gamma_V-a_I)-a_{HL}a_F a_{IF}(b_{HD}H_{max})^2}{a_{HL}^2 b_{FI}(\alpha_{VH}+a_{VH})}$, $F^*=\frac{b_{HD}H_{max}}{a_{HL}}$ and $H^*=(\frac{a_{HL}b_{FI}-a_{HF}b_{HD}-a_{HF}b_{FI}}{a_{HL}b_{FI}}-\gamma_{HV}\frac{b_{FI}a_{HL}(\gamma_V-a_I)-a_{HL}a_F a_{IF}(b_{HD}H_{max})}{a_{HL}^2 b_{FI}(\alpha_{VH}+a_{VH})})H_{max}$.
- Associated to LRT: $E_5=(0,0,0,H_L^*,I_L^*,V_L^*,F^*)$, where $I_L^*=\frac{a_F b_{HD}H_{max}}{a_{HF}b_{FI}}$, $V_L^*=\frac{b_{HD}H_{max}(\gamma_V a_{HF}-a_{IF}b_{HD}H_{max}-a_I a_{HF})}{a_{HF}^2 b_{FI}(\alpha_{VL}+a_{VL}+\beta)}$, $F^*=\frac{b_{HD}H_{max}}{a_{HF}}$ and $H_L^*=\left[\frac{a_{HF}b_{FI}-a_F b_{HD}-a_{HL}b_{FI}}{a_{HF}b_{FI}}-a_F\gamma_{HV}\frac{(\gamma_V a_{HF}-a_{IF}b_{HD}H_{max}-a_I a_{HF})}{a_{HF}^2 b_{FI}(\alpha_{VL}+a_{VL}+\beta)}\right]H_{max}$.
- Associated to both URT and LRT: it is in the form $E_6=(H_U^*,I_U^*,V_U^*,H_L^*,I_L^*,V_L^*,F^*)$.

2.2. Basic reproduction number

It is an important parameter used in epidemiology to predict the asymptotic state of the infection. It measures the average number of secondary infections caused by a single infected when introduced in a population of purely susceptible. It is computed using the next generation matrix approach as follows: let

$$\mathcal{F}=\begin{pmatrix}0\\ \gamma_{HV}V_U H_U\\ 0\\ \gamma_{HV}V_L H_L\end{pmatrix}\text{ and }\mathcal{V}=\begin{pmatrix}-\gamma_V I_U+\gamma_{VH}H_U V_U+\alpha_{VH}V_U+a_{VH}V_U-\beta V_L\\ a_{IF}FI_U+a_I I_U\\ -\gamma_V I_L+\gamma_{VH}H_L V_L+\alpha_{VL}V_L+a_{VH}V_L+\beta V_L\\ a_{IF}FI_L+a_I I_L\end{pmatrix} \tag{2.10}$$

be the vectors representing new infections, and the disease progression, death and recovery, respectively.

2.2.1. Case associated with URT

We have

$$\mathcal{F}_1=\begin{pmatrix}0\\ \gamma_{HV}V_U H_U\end{pmatrix}\text{ and }\mathcal{V}_1=\begin{pmatrix}-\gamma_V I_U+\gamma_{VH}H_U V_U+\alpha_{VH}V_U+a_{VH}V_U-\beta V_L\\ a_{IF}FI_U+a_I I_U\end{pmatrix}. \tag{2.11}$$

This implies that

$$F_1=\frac{\partial\mathcal{F}(E_1)}{\partial(V_U,I_U,V_L,I_L)}=\begin{pmatrix}0&0\\ \gamma_{HV}H_{max}&0\end{pmatrix}, \tag{2.12}$$

$$V_1=\frac{\partial\mathcal{V}_1(E_1)}{\partial(V_U,I_U,V_L,I_L)}=\begin{pmatrix}\gamma_{VH}H_{max}+\alpha_{VH}+a_{VH}&-\gamma_V\\ 0&a_I\end{pmatrix}. \tag{2.13}$$

The next generation matrix is given by

$$F_1V_1^{-1}=\frac{1}{a_I\gamma_{VH}H_{max}+\alpha_{VH}+a_{VH}}\begin{pmatrix}0&0\\ \gamma_{HV}H_{max}a_I&\gamma_V\gamma_{HV}H_{max}\end{pmatrix}, \tag{2.14}$$

and has two eigenvalues $\lambda_1=0$ et $\lambda_2=\frac{\gamma_V\gamma_{HV}H_{max}}{a_I(\gamma_{HV}H_{max}+\alpha_{VH}+a_{VH})}$. Therefore the basic reproduction number is

$$\mathcal{R}_1=\max\{\lambda_1,\lambda_2\}=\frac{\gamma_V\gamma_{HV}H_{\max}}{a_I(\gamma_{HV}H_{max}+\alpha_{VH}+a_{VH})}. \tag{2.15}$$

2.2.2. Case associated to LRT

Likewise

$$\mathcal{F}_2 = \begin{pmatrix} 0 \\ \gamma_{HV} V_L H_L \end{pmatrix} \text{ and } \mathcal{V}_2 = \begin{pmatrix} -\gamma_V I_L + \gamma_{VH} H_L V_L + \alpha_{VL} V_L + a_{VL} V_L + \beta V_L \\ a_{IF} F I_L + a_I I_L \end{pmatrix}. \tag{2.16}$$

Thus

$$F_2 = \frac{\partial \mathcal{F}_2(E_2)}{\partial(V_U, I_U, V_L, I_L)} = \begin{pmatrix} 0 & 0 \\ \gamma_{HV} H_{max} & 0 \end{pmatrix}, \tag{2.17}$$

$$V_2 = \frac{\partial \mathcal{V}_2(E_2)}{\partial(V_U, I_U, V_L, I_L)} = \begin{pmatrix} \gamma_{VH} H_{max} + \alpha_{VL} + a_{VL} & -\gamma_V \\ 0 & a_I \end{pmatrix}. \tag{2.18}$$

The next generation matrix is

$$F_2 V_2^{-1} = \frac{1}{a_I \gamma_{VH} H_{max} + \alpha_{VL} + a_{VL} + \beta} \begin{pmatrix} 0 & 0 \\ \gamma_{HV} H_{max} a_I & \gamma_{HV} H_{max} \end{pmatrix}. \tag{2.19}$$

As a result, the basic reproduction number is given by

$$\mathcal{R}_2 = \frac{\gamma_V \gamma_{HV} H_{\max}}{a_I(\gamma_{HV} H_{max} + \alpha_{VL} + a_{VL} + \beta)}. \tag{2.20}$$

2.2.3. Case associated to both URT and LRT

The basic reproduction number is given by

$$\mathcal{R}_0 = \max(\mathcal{R}_1, \mathcal{R}_2), \tag{2.21}$$

where $\mathcal{R}_1$ and $\mathcal{R}_2$ are given by (2.15) and (2.20) respectively.

2.3. Stability analysis

The characteristic polynomial at a point $E^* = (H_U^*, I_U^*, V_U^*, H_L^*, I_L^*, V_L^*, F^*)$ is

$$P(\lambda) = \det(A_{E^*}) = \det(\lambda I - J_{E^*} - J_{E^*}^r e^{-\lambda\tau}), \tag{2.22}$$

where J_{E^*} and $J_{E^*}^r$ are Jacobian matrices associated to the terms without and with delay, respectively. They are given by

$$J_{E^*} = \begin{bmatrix} \alpha_1 & -\gamma_{VH} H_U^* & \gamma_V & \beta & 0 & 0 & 0 \\ -\gamma_{VH} H_U^* & \alpha_2 & -b_{HD} H_U^* & 0 & 0 & 0 & -a_{HF} H_U^* \\ 0 & 0 & \alpha_5 & 0 & 0 & 0 & -a_{IF} I_U^* \\ 0 & 0 & 0 & \alpha_3 & -\gamma_{VH} V_L^* & \gamma_V & 0 \\ 0 & 0 & 0 & -\gamma_{VH} H_L & \alpha_4 & -b_{HD} H_L & -a_{HL} H_L \\ 0 & 0 & 0 & 0 & 0 & \alpha_6 & -a_{IF} I_L^* \\ 0 & 0 & b_{FI} & 0 & 0 & b_{FI} & -a_F \end{bmatrix} \tag{2.23}$$

and

$$J_{E^*}^r = \begin{bmatrix} 0 & 0 & 0 & 0 & 0 & 0 & 0 \\ 0 & 0 & 0 & 0 & 0 & 0 & 0 \\ -\gamma_{HV} H_{U\tau}^* & -\gamma_{HV} V_{U\tau}^* & 0 & 0 & 0 & 0 & 0 \\ 0 & 0 & 0 & 0 & 0 & 0 & 0 \\ 0 & 0 & 0 & 0 & 0 & 0 & 0 \\ 0 & 0 & 0 & -\gamma_{HV} H_{L\tau}^* & -\gamma_{HV} V_{L\tau}^* & 0 & 0 \\ 0 & 0 & 0 & 0 & 0 & 0 & 0 \end{bmatrix}, \tag{2.24}$$

with $\alpha_1 = -\gamma_{VH} H_U - \alpha_{VH} - a_{VH}$, $\alpha_2 = b_{HD} H_{max} - 2b_{HD} H_U - b_{HD} I_U - \gamma_{VH} V_U - a_{HF} F$, $\alpha_3 = b_{HD} H_{max} - 2b_{HD} H_L - b_{HD} I_L - \gamma_{VH} V_L - a_{HL} F$, $\alpha_4 = -\gamma_{VH} H_L - \alpha_{VH} - a_{VH} - \beta.$, $\alpha_5 = -a_{HF} F^* - a_I$ and $\alpha_6 = -a_I - a_{IF} F^*$.

Theorem 2.1. *The equilibrium points E_0, E_1 and E_2 are unstable.*

Proof. It can easily be checked that $\lambda = b_{HD} H_{\max} > 0$ is an eigenvalue of the matrices A_{E_0}, A_{E_1} and A_{E_2}. □

The instability of E_0, E_1 and E_2 reveal that epithelial cells cannot be completely cleared-off in either respiratory tracks.

Theorem 2.2. *The equilibrium point E_3 is stable when $\mathcal{R}_0 = \max\{\mathcal{R}_1, \mathcal{R}_2\} \leq 1$.*

Proof. The characteristic polynomial is given by

$$p(\lambda) = \det(\lambda I - J_{E_3} - J_{E_3}^r e^{-\lambda\tau}), \tag{2.25}$$

$$= \begin{vmatrix} \lambda+m_3 & 0 & \gamma_V & -\beta & 0 & 0 & 0 \\ \gamma_{VH}H_{max} & \lambda+\alpha & \alpha & 0 & 0 & 0 & a_{HF}H_{max} \\ m_4 & 0 & \lambda+a_I & 0 & 0 & 0 & 0 \\ 0 & 0 & 0 & \lambda+n_3 & 0 & -\gamma_V & 0 \\ 0 & 0 & 0 & \gamma_{VH}H_{max} & \lambda+\alpha & -\alpha & -a_{HL}H_{max} \\ 0 & 0 & 0 & m_4 & 0 & \lambda+a_I & 0 \\ 0 & 0 & -b_{FI} & 0 & 0 & -b_{FI} & \lambda+a_F \end{vmatrix} \tag{2.26}$$

where $m_3 = \gamma_{VH}H_{max} + \alpha_{VH} + a_{VH}$, $m_4 = \gamma_{VH}H_{max}e^{-\lambda\tau}$, $n_3 = \gamma_{VH}H_{max} + \alpha_{VH} + a_{VH} + \beta$ and $\alpha = b_{HD}H_{max}$. We observe that $\lambda_1 = \lambda_2 = -\alpha = -b_{HD}H_{max}$ and $\lambda_3 = -a_F$ are zeros of $p(\lambda)$, and are negative. Then, $p(\lambda) = (\lambda-\lambda_1)^2(\lambda-\lambda_3)p_0(\lambda)$, with

$$p_0(\lambda) = \left|\begin{array}{cc|cc} \lambda+m_3 & \gamma_V & -\beta & 0 \\ \gamma_{VH}H_{max}e^{-\lambda\tau} & \lambda+a_I & 0 & 0 \\ \hline 0 & 0 & \lambda+n_3 & -\gamma_V \\ 0 & 0 & \gamma_{VH}H_{max}e^{-\lambda\tau} & \lambda+a_I \end{array}\right| \tag{2.27}$$

$$= p_1(\lambda)p_2(\lambda), \tag{2.28}$$

where

$$p_1(\lambda) = (\lambda+m_3)(\lambda+a_I) - \gamma_V m_4 = (\lambda+m_3)(\lambda+a_I) - a_I m_3 \mathcal{R}_1 e^{-\lambda\tau} \tag{2.29}$$

$$p_2(\lambda) = (\lambda+n_3)(\lambda+a_I) - \gamma_V m_4 = (\lambda+n_3)(\lambda+a_I) - a_I n_3 \mathcal{R}_2 e^{-\lambda\tau}. \tag{2.30}$$

Let λ be a zero of $p_1(\lambda)$. Then $(\lambda+m_3)(\lambda+a_I) = a_I m_3 \mathcal{R}_1 e^{-\lambda\tau}$.

i. Assume $\mathcal{R}_1 < 1$. If $\mathcal{R}_e(\lambda) \geq 0$, then $e^{-\mathcal{R}_e(\lambda)\tau} \leq 1$ and

$$a_I m_3 \leq (|\lambda+a_I|)(|\lambda+m_3|) = a_I m_3 \mathcal{R}_1 |e^{-\lambda\tau}| \leq a_I m_3 \mathcal{R}_1. \tag{2.31}$$

This implies that $\mathcal{R}_1 \geq 1$ and contradict the hypothesis $\mathcal{R}_0 < 1$. Thus, the real part of the zeros of $p_1(\lambda)$ is negative when $\mathcal{R}_1 < 1$.

ii. For $\mathcal{R}_1 = 1$, if $\mathcal{R}_e(\lambda) > 0$, then

$$a_I m_3 \leq (|\lambda+a_I|)(|\lambda+m_3|) \leq a_I m_3 \mathcal{R}_1 e^{-\mathcal{R}_e(\lambda)\tau} = a_I m_3 e^{-\mathcal{R}_e(\lambda)\tau}. \tag{2.32}$$

This implies that $e^{-\mathcal{R}_e(\lambda)\tau} \geq 1$ and contradicts the hypothesis that $\mathcal{R}_e(\lambda) > 0$.

In the same manner, one can show that the real part of the zeros of $p_2(\lambda)$ is negative when $\mathcal{R}_2 \leq 1$. From which the stability of E_3 when $\mathcal{R}_0 = \max\{\mathcal{R}_1, \mathcal{R}_2\} \leq 1$. □

Theorem 2.3. *When $\mathcal{R}_0 = \max\{\mathcal{R}_1, \mathcal{R}_2\} > 1$, a Hopf bifurcation occurs.*

Proof. We assume $\mathcal{R}_1 > 1$ and $\lambda \in \mathbb{R}$. Since $p_1(0) = a_I m_3(1-\mathcal{R}_1) < 0$ and $\lim_{\lambda \longrightarrow +\infty} p_1(\lambda) = +\infty$, there exists $\lambda_0 > 0$ such that $p_1(\lambda_0) = 0$. In the same manner, one can show that at least a zero of $p_2(\lambda)$ is positive. In this case, E_3 is unstable.

Let $\lambda \in \mathbb{C}$ be a root of $p_1(\lambda)$. At the Hopf bifurcation point, λ is purely imaginary and in the form $\lambda = iw_1$, where $w_1 \in \mathbb{R}^*$. From (2.29), we have

$$(iw_1+a_I)(iw_1+m_3) = a_I m_3 \mathcal{R}_1 e^{-iw_1\tau}, \tag{2.33}$$

which implies that

$$-w_1^2 + iw_1(a_I+m_3) + a_I m_3 = a_I m_3 \mathcal{R}_1[cos(w_1\tau) - sin(w_1\tau)]. \tag{2.34}$$

We obtain the system

$$\begin{cases} a_I m_3 \mathcal{R}_1 \cos(w_1\tau) &= a_I m_3 - w_1^2 \\ a_I m_3 \sin(w_1\tau) &= -w_1(a_I+m_3) \end{cases} \tag{2.35}$$

As a result,

$$a_I^2 m_3^2 \mathcal{R}_1^2 = (a_I m_3 - w_1^2)^2 + w_1^2(a_I+m_3)^2. \tag{2.36}$$

Expanding, we get

$$w_1^4 + (a_I^2+m_3^2)w_1^2 + a_I^2 m_3^2(1-\mathcal{R}_1^2) = 0. \tag{2.37}$$

This yields the solution

$$w_1 = \pm\sqrt{\frac{1}{2}\left[-(a_I^2+m_3^2) + \sqrt{(a_I^2+m_3^2)^2 + 4a_I^2 m_3^2(\mathcal{R}_1^2-1)}\right]}. \tag{2.38}$$

In the same manner, the polynomial $p_2(\lambda)$ has purely imaginary roots $\lambda = iw_2$ where

$$w_2 = \pm\sqrt{\frac{1}{2}\left[-(a_I^2+n_3^2) + \sqrt{(a_I^2+n_3^2)^2 + 4a_I^2 n_3^2(\mathcal{R}_1^2-1)}\right]}. \tag{2.39}$$

Table 2
Sensitivity index of $\mathcal{R}_1$ and $\mathcal{R}_2$ with respect to some model parameters.

x	γ_V	a_I	α_I	H_{max}	γ_{VH}	α_{VH}	a_{VH}	β
$\frac{\partial \mathcal{R}_1}{\partial x} \times \frac{x}{\mathcal{R}_1}$	1	-1	0	0.0387	-0.96	−0.0018	−0.0368	0
$\frac{\partial \mathcal{R}_2}{\partial x} \times \frac{x}{\mathcal{R}_2}$	1	-1	0	0.0432	0	0	0	-5.4×10^{-5}

Hence, the occurrence of the Hopf bifurcation. □

From the above theorem, we note the possibility to overcome the infection when $\mathcal{R}_0 > 1$. This observation is not possible when delay is not considered. The latency period plays an important role in the control of the infection dynamics. We will later illustrate this numerically.

2.4. Sensitivity analysis

As indicated in Theorem 2.2, the infection-free equilibrium can be reached when $\mathcal{R}_0 < 1$. We investigate in the section some strategies to reduce $\mathcal{R}_0$ by looking at the influence of some parameters on $\mathcal{R}_0$.

- The absolute sensitivity of $\mathcal{R}_1$ and $\mathcal{R}_2$ with respect to γ_V, γ_{HV} et H_{max} are positives and given by

$$\frac{\partial \mathcal{R}_1}{\partial \gamma_V} = \frac{\gamma_{HV} H_{max}}{a_I(\gamma_{VH} H_{max} + \alpha_{VH} + a_{VH})}, \tag{2.40}$$

$$\frac{\partial \mathcal{R}_1}{\partial \gamma_{HV}} = \frac{\gamma_V H_{max}}{a_I(\gamma_{VH} H_{max} + \alpha_{VH} + a_{VH})}, \tag{2.41}$$

$$\frac{\partial \mathcal{R}_2}{\partial \gamma_V} = \frac{\gamma_{HV} H_{max}}{a_I(\gamma_{HV} H_{max} + \alpha_{VL} + a_{VL} + \beta)}, \tag{2.42}$$

$$\frac{\partial \mathcal{R}_2}{\partial \gamma_{HV}} = \frac{\gamma_V H_{max}(\gamma_{HV} H_{max} + \alpha_{VL} + a_{VL} + \beta) - \gamma_{HV} H_{max}^2}{a_I(\gamma_{VH} H_{max} + \alpha_{VU} + a_{VU})^2} \tag{2.43}$$

$$\frac{\partial \mathcal{R}_1}{\partial H_{max}} = \frac{\gamma_V \gamma_{HV} a_I(\alpha_{VH} + a_{VH})}{a_I^2(\gamma_{VH} H_{max} + \alpha_{VH} + a_{VH})^2}, \tag{2.44}$$

$$\frac{\partial \mathcal{R}_2}{\partial H_{max}} = \frac{\gamma_V \gamma_{HV}(\alpha_{VL} + a_{VL})}{a_I(\gamma_{VH} H_{max} + \alpha_{VH} + a_{VH})^2}. \tag{2.45}$$

  Therefore reducing the replication rate γ_V of virus, or infection rate γ_{HV} of cells, or the carrying capacity H_{max} of cells will reduce secondary infections.
- Likewise, the absolute sensitivity of $\mathcal{R}_1$ et $\mathcal{R}_2$ with respect to a_I, γ_{VH}, a_{VH} and β are negative. As a result, increasing the mortality rate a_I of infected cells, or the absorption rate γ_{HV} of the virus by healthy cells, or the destruction rate a_{VH} of virus by a non specific immunity, or the migration rate β of virus, will decrease secondary infections.

The absolute sensitivity analysis provides strategies to reduce $\mathcal{R}_0$, but does not inform on the specific contributions of each parameter. In Table 2, we computed the sensitivity index of $\mathcal{R}_0$ with respect to some parameters. We used the values: $\gamma_V = 3459 \times 10^6$, $\gamma_{VH} = 3.1792$, $a_{VH} = 6.0624$, $\alpha_{VH} =$, $\beta = 5.4065 \times 10^{-2}$, $b_{HD} = 43910$, $\gamma_{HV} = 7.6059 \times 10^{-8}$, $a_{HF} = 0.0099$, $a_{IF} = 0.0126$, $a_I = 4.4981$, $a_{VL} = 431.59$, $\alpha_{VL} = 0.0014$, $b_{FI} = 0.0078$, $H_{max} = 50$ [23].

We observe that reducing by 10% the replication rate γ_V of virus or the carrying capacity H_{max}, will decrease $\mathcal{R}_1$ to 10% or 0.387% respectively. Increasing by 10% the absorption rate γ_{VH} of virus by cells, or the destruction rates α_{VH}, a_{VH} of virus, or the mortality rate a_I, will decrease $\mathcal{R}_1$ to respectively 9.6%, 0.0187, 0.368% or 10%. We also observe that the absorption rate of viruses by cells or the rates α_{VH}, a_{VH} has no effect on secondary infections associated with LRT. Therefore, reducing the replication rate of virus, or increasing the death rate of infected cells or absorption of virus by cells are in this case the best strategies to reduce secondary infections.

The implementation of these strategies required costs. In the next section, we will investigate the optimal cost to reduce secondary infections.

3. Optimal control model with delay

We consider two control parameters: u_1 for the efficacy of the treatment in preventing new infections and u_2 for the efficacy of the treatment in inhibiting viral production (with $0 \le u_1, u_2 \le 1$). The objective of this section is to determine the control $u(t) = (u_1(t), u_2(t))$ which minimizes the cost function:

$$J(u) = \int_0^T [a_1 I_U(t) + a_2 V_U(t) + a_3 I_L(t) + a_4 V_L(t) + \frac{1}{2}(A_1 u_1^2(t) + A_2 u_2^2(t))]dt. \tag{3.1}$$

We define the optimal control problem which consists to

$$\text{minimize } J(u),\ u \in U \tag{3.2}$$

subjected to the state system

$$\frac{dV_U(t)}{dt} = (1 - u_2(t))\gamma_V I_U(t) - \gamma_{VH} V_U(t) H_U(t) - \alpha_{VH} V_U(t) - a_{VH} V_U(t) + \beta V_L(t) = g_1 \tag{3.3}$$

$$\frac{dH_U(t)}{dt} = b_{HD}(H_{max} - H_U(t) - I_U(t))H_U(t) - (1-u_1(t))\gamma_{HV}V_U(t)H_U(t) - a_{HF}F(t)H_U(t) = g_2 \tag{3.4}$$

$$\frac{dI_U(t)}{dt} = (1-u_1(t-\tau))\gamma_{HV}V_U(t-\tau)H_U(t-\tau) - a_{IF}F(t)I_U(t) - a_I I_U(t) = g_3 \tag{3.5}$$

$$\frac{dV_L(t)}{dt} = (1-u_2(t))\gamma_V I_L(t) - \gamma_{VH}V_L(t)H_L(t) - \alpha_{VH}V_L(t) - a_{VH}V_L(t) - \beta V_L(t) = g_4 \tag{3.6}$$

$$\frac{dH_L(t)}{dt} = b_{HD}(H_{max} - H_L(t) - I_L(t))H_L(t) - (1-u_1(t))\gamma_{HV}V_L(t)H_L(t) - a_{HF}F(t)H_L(t) = g_5 \tag{3.7}$$

$$\frac{dI_L(t)}{dt} = (1-u_1(t-\tau))\gamma_{HV}V_L(t-\tau)H_L(t-\tau) - a_{IF}F(t)I_L(t) - a_I I_L(t) = g_6 \tag{3.8}$$

$$\frac{dF(t)}{dt} = b_{FI}(I_U(t) + I_L(t)) - a_F F(t) = g_7, \tag{3.9}$$

where $U = \{u = (u_1, u_2) : [0,T] \to [0,1] \times [0,1]$ measurable function$\}$. In (3.1), we note that the linear terms represent infected cells and virus, the quadratic terms in u_1 and u_2 represent the treatment and physiological costs respectively, and T is the set time for treatment. The constants a_1, a_2, a_3, a_4, A_1 and A_2 are non-negative. We consider quadratic terms in u_1 and u_2 to avoid a bang-bang control solution. Our control problem consists in minimizing cell infection and viruses, at an optimal cost. The implementation of this control strategy will require investment in research to produce an effective treatment. The elimination of the infection is not the target, though it is the ideal situation. However, it aims to improve the state of the infected individuals at an optimal cost.

3.1. Existence of an optimal solution

We establish the existence of the optimal solution of the system (3.2)-(3.9) using the result of Fleming and Rishel [9].

Theorem 3.1. *There exists an optimal solution* $(x^*, u^*) \in \mathbb{R}^7 \times U$ *of the control problem* (3.2)-(3.9) *such that*

$$J(u^*) = \min_{u \in U} J(u) \tag{3.10}$$

where $x^* = (V_U^*, H_U^*, I_U^*, V_L^*, H_L^*, I_L^*, F^*)^T$.

Proof. It suffices to verify that the conditions of Fleming and Rishel [9] hold.

- Since $g = (g_1, ..., g_7)$ is a polynomial function, it is of class C^1. By applying the Cauchy-Picard theorem, there is a local solution. Consequently, the set of admissible states is non-empty.
- By definition, the admissible control set U is closed and convex.
- Keeping the positive terms, according to the system (3.3)-(3.9) we have:

$$\begin{cases} g_1 < (1-u_2)\gamma_V I_U(t) + \beta V_L(t) \\ g_2 < b_{HD}H_{max}H_U(t) \\ g_3 < (1-u_1)\gamma_{HV}V_U(t-\tau)H_U(t-\tau) \\ g_4 < (1-u_2)\gamma_V I_L(t) \\ g_5 < b_{HD}H_{max}H_L(t) \\ g_6 < (1-u_1)\gamma_{HV}V_L(t-\tau)H_L(t-\tau) \\ g_7 < b_{FI}(I_U(t) + I_L(t)). \end{cases} \tag{3.11}$$

This implies that

$$\begin{aligned} ||g(x(t), x(t-\tau), u(t)||_1 &\le ||g_1||_1 + ||g_2||_1 + ||g_3||_1 + ||g_4||_1 + ||g_5||_1 + ||g_6||_1 + ||g_7||_1 \\ &\le C_1 h(x(t)) + C_2 h(x(t-\tau)) \end{aligned}$$

where $h(x(t)) = ||I_U(t)||_1 + ||V_L(t)||_1 + ||H_U(t)||_1 + ||I_L(t)||_1 + ||H_L(t)||_1$, $h(x(t-\tau)) = ||V_U(t-\tau)H_U(t-\tau)||_1 + ||V_L(t-\tau)H_L(t-\tau)||_1$, $C_1 = \min(\gamma_V, \beta, b_{HD}H_{max}, b_{FI})$ and $C_2 = \gamma_{HV}$.

- The integrand $f(x(t), u(t)) = a_1 I_U(t) + a_2 V_U(t) + a_3 I_L(t) + a_4 V_L(t) + \frac{1}{2}(A_1 u_1^2(t) + A_2 u_2^2(t))$ is convex (since it is a positive quadratic function). Moreover,

$$f(x(t), u(t)) \ge \frac{1}{2}(A_1 u_1^2(t) + A_2 u_2^2(t)) \ge C_1(|u_1|^2 + |u|^2)^{\frac{\beta}{2}} - C_2 \tag{3.12}$$

with $C_1 = \frac{1}{2}\min(A_1, A_1)$, $C_2 > 0$ and $\beta = 2$.

Since the Fleming and Rishel hypotheses hold, there exists an optimal control $u^* = (u_1^*, u_2^*)$ minimizing the objective function (3.2) subjected to the system (3.3)-(3.9). □

3.2. Characterization of the optimal control

We will use a maximum principle of Pontryagin type which was derived by Gollman for optimal control problems with delays [11]. We define the Lagragian by:

$$L(x, x_\tau, u, \lambda)(t) = f(x(t), u(t)) + < \lambda(t); g(x(t), x_\tau(t), u(t), \lambda(t)) > \\ -r_{11}u_1 - r_{12}(1-u_1) - r_{21}u_2 - r_{22}(1-u_2), \tag{3.13}$$

where $< .,. >$ is the Euclidean scalar product, $u = (u_1, u_2)$, $x_\tau(t) = x(t-\tau)$ and the $r_{ij} \geq 0$ (for all $i, j \in \{1, 2\}$) are penalty multipliers ensuring the boundedness of the control between 0 and 1, and satisfying:

$$r_{11}u_1 = r_{12}(1-u_1) = 0 \tag{3.14}$$

$$r_{21}u_2 = r_{22}(1-u_2) = 0. \tag{3.15}$$

Theorem 3.2. *Let $u^* = (u_1^*, u_2^*)$ be the optimal control corresponding to the optimal solution $x^* = (V_U^*, H_U^*, I_U^*, V_L^*, H_L^*, I_L^*, F^*)$ of system (3.2)-(3.9). Then there exists $\lambda_i(t)$, $i \in \{1, 2, 3, 4, 5, 6, 7\}$, satisfying:*

$$-\frac{d\lambda_1}{dt} = a_2 - \lambda_1(\gamma_{VH}H_U + \alpha_{VH} + a_{VH}) - \lambda_2\gamma_{HV}(1-u_1)H_U + \lambda_{1\tau}\lambda_3\gamma_{HV}(1-u_1)H_{U\tau} \tag{3.16}$$

$$-\frac{d\lambda_2}{dt} = -\lambda_1\gamma_{VH}V_U - \lambda_2(b_{HD}(2H_U - H_{max} + I_U) + \gamma_{HV}(1-u_1)V_U + a_{HF}F) \\ +\lambda_{2\tau}\lambda_3\gamma_{HV}(1-u_1)V_{U\tau} \tag{3.17}$$

$$-\frac{d\lambda_3}{dt} = a_1 + \lambda_1\gamma_V(1-u_2) - \lambda_2 b_{HD}H_U - \lambda_3(a_{IF}F + a_I) + \lambda_7 b_{FI} \tag{3.18}$$

$$-\frac{d\lambda_4}{dt} = a_4 + \lambda_1\beta - \lambda_4(\gamma_{VH}H_L + \alpha_{VH} + a_{VH} + \beta) - \lambda_5\gamma_{HV}(1-u_1)H_L \\ +\lambda_{4\tau}\lambda_6\gamma_{HV}(1-u_1)H_{L\tau} \tag{3.19}$$

$$-\frac{d\lambda_5}{dt} = -\lambda_4\gamma_{VH}V_L - \lambda_5(b_{HD}(2H_L - H_{max} + I_L) + \gamma_{HV}(1-u_1)V_L + a_{HF}F) \\ +\lambda_{5\tau}\lambda_6\gamma_{HV}(1-u_1)V_{L\tau} \tag{3.20}$$

$$-\frac{d\lambda_6}{dt} = a_3 + \lambda_4\gamma_V(1-u_2) - \lambda_5 b_{HD}H_L - \lambda_6(a_{IF}F + a_I) + \lambda_7 b_{FI} \tag{3.21}$$

$$-\frac{d\lambda_7}{dt} = -\lambda_2 a_{HF}H_U - \lambda_3 a_{IF}I_U - \lambda_5 a_{HF}H_L - \lambda_6 a_{IF}I_L - \lambda_7 a_F \tag{3.22}$$

with boundary conditions

$$\lambda_i(T) = 0, \quad i = 1, \ldots, 7. \tag{3.23}$$

Moreover, the control u^* verifies:

$$u_1^* = \max\left\{0, \min\left(1, \frac{\gamma_{HV}(\lambda_3 V_{U\tau}H_{U\tau} - \lambda_6 V_{L\tau}H_{L\tau}) - (\lambda_2 V_U H_U + \lambda_5 V_L H_L)}{A_1}\right)\right\} \tag{3.24}$$

$$u_2^* = \max\left\{0, \min\left(1, \frac{\lambda_1\gamma_V I_U + \lambda_4\gamma_V I_L}{A_2}\right)\right\}. \tag{3.25}$$

Proof. The system (3.16)-(3.22) is obtained by substituting the Lagrangian (3.13) in the system

$$-\frac{d\lambda_1}{dt} = \frac{\partial L}{\partial V_U} + \lambda_1(t+\tau)\frac{\partial L}{\partial V_{U\tau}} \tag{3.26}$$

$$-\frac{d\lambda_2}{dt} = \frac{\partial L}{\partial H_U} + \lambda_2(t+\tau)\frac{\partial L}{\partial H_{U\tau}} \tag{3.27}$$

$$-\frac{d\lambda_3}{dt} = \frac{\partial L}{\partial I_U} + \lambda_3(t+\tau)\frac{\partial L}{\partial I_{U\tau}} \tag{3.28}$$

$$-\frac{d\lambda_4}{dt} = \frac{\partial L}{\partial V_L} + \lambda_4(t+\tau)\frac{\partial L}{\partial V_{L\tau}} \tag{3.29}$$

$$-\frac{d\lambda_5}{dt} = \frac{\partial L}{\partial H_L} + \lambda_5(t+\tau)\frac{\partial L}{\partial H_{L\tau}} \tag{3.30}$$

$$-\frac{d\lambda_6}{dt} = \frac{\partial L}{\partial I_L} + \lambda_6(t+\tau)\frac{\partial L}{\partial I_{L\tau}} \tag{3.31}$$

$$-\frac{d\lambda_7}{dt} = \frac{\partial L}{\partial F} + \lambda_7(t+\tau)\frac{\partial L}{\partial F\tau}. \tag{3.32}$$

It is a system of non-autonomous first-order linear ordinary differential equations in λ of the form $\lambda' = A(t)R + B(t)$. The coefficients $A(t)$ and $B(t)$ being continuous, according to the Cauchy-Picard theorem, there exists a solution $\lambda(t)$ satisfying this system.
The optimality condition $L_u = 0$ will allow us to find the optimal controls. We have

$$\frac{\partial L}{\partial u_1^*} = A_1 u_1^* + \lambda_2 \gamma_{HV} V_U H_U - \lambda_3 \gamma_{HV} V_{U\tau} H_{U\tau} + \lambda_5 \gamma_{HV} V_L H_L - \lambda_6 \gamma_{HV} V_{L\tau} H_{L\tau}$$
$$-r_{11} + r_{12} = 0 \tag{3.33}$$
$$\frac{\partial L}{\partial u_2^*} = A_2 u_2^* - \lambda_1 \gamma_V I_U - \lambda_4 \gamma_V I_L - r_{21} + r_{22} = 0. \tag{3.34}$$

This implies that

$$u_1^* = \frac{(\gamma_{HV}(\lambda_3 V_{U\tau} H_{U\tau} - \lambda_6 V_{L\tau} H_{L\tau}) - (\lambda_2 V_U H_U + \lambda_5 V_L H_L)) + r_{11} - r_{12}}{A_1} \tag{3.35}$$
$$u_2^* = \frac{\lambda_1 \gamma_V I_U + \lambda_4 \gamma_V I_L + r_{21} - r_{22}}{A_2}. \tag{3.36}$$

To obtain an explicit formula of the optimal controls without the r_{ij}, we use standard techniques. We consider three cases:

- Let $\{t : 0 < u_1^* < 1\}$ be the set. Since by definition $r_{11} u_1^* = r_{12}(1 - u_1^*) = 0$, then $r_{11} = r_{12} = 0$. Therefore,
$$u_1^* = \frac{(\gamma_{HV}(\lambda_3 V_{U\tau} H_{U\tau} - \lambda_6 V_{L\tau} H_{L\tau}) - (\lambda_2 V_U H_U + \lambda_5 V_L H_L))}{A_1} < 1. \tag{3.37}$$
- In the set $\{t : u_1^* = 1\}$, we have $r_{11} = 0$ and
$$1 = u_1^* = \frac{(\gamma_{HV}(\lambda_3 V_{U\tau} H_{U\tau} - \lambda_6 V_{L\tau} H_{L\tau}) - (\lambda_2 V_U H_U + \lambda_5 V_L H_L)) - r_{12}}{A_1}. \tag{3.38}$$
Therefore,
$$\frac{(\gamma_{HV}(\lambda_3 V_{U\tau} H_{U\tau} - \lambda_6 V_{L\tau} H_{L\tau}) - (\lambda_2 V_U H_U + \lambda_5 V_L H_L))}{A_1} \geq 1 \tag{3.39}$$
because $r_{12} > 0$ from the definition.
- In the set $\{t : u_1^* = 0\}$, we have $r_{12} = 0$ and
$$0 = u_1^* = \frac{(\gamma_{HV}(\lambda_3 V_{U\tau} H_{U\tau} - \lambda_6 V_{L\tau} H_{L\tau}) - (\lambda_2 V_U H_U + \lambda_5 V_L H_L)) + r_{11}}{A_1}. \tag{3.40}$$
Thus,
$$\frac{(\gamma_{HV}(\lambda_3 V_{U\tau} H_{U\tau} - \lambda_6 V_{L\tau} H_{L\tau}) - (\lambda_2 V_U H_U + \lambda_5 V_L H_L))}{A_1} \leq 0. \tag{3.41}$$

We thus obtain

$$u_1^* = \max\left\{0, \min\left(1, \frac{(\gamma_{HV}(\lambda_3 V_{U\tau} H_{U\tau} - \lambda_6 V_{L\tau} H_{L\tau}) - (\lambda_2 V_U H_U + \lambda_5 V_L H_L))}{A_1}\right)\right\}. \tag{3.42}$$

In the same manner, it can be shown that

$$u_2^* = \max\left\{0, \min\left(1, \frac{\lambda_1 \gamma_V I_U + \lambda_4 \gamma_V I_L}{A_2}\right)\right\}. \quad \square \tag{3.43}$$

4. Numerical simulations

We graphically illustrate the theoretical results using the experimental data [23]: $\gamma_{VH} = 3.179$, $\alpha_{VH} = 0.3077$, $\beta = 0.0540$, $H_{max} = 50$, $\gamma_{HV} = 0.00000076$, $a_{HF} = 0.0099$, $a_{IF} = 0.0126$, $a_I = 4.498$, $\alpha_{VL} = 0.0014$, $a_{VH} = 6.062$, $b_{FI} = 0.0078$, $a_F = 10.250$, $a_{VL} = 431.59$, et $a_{HL} = 40$. To illustrate the scenarios of epidemic and endemic infection, we used in the Figs. 1-4: $\gamma_V = 345900$, $b_{HD} = 0.43910$, $I_U(0) = 20$, $I_L(0) = 15$, $F(0) = 100$, $V_U(t) = 10$, $H_U(t) = 10$, $V_L(t) = 10$, $H_L(t) = 10$ for all $t \in [-\tau, 0]$ ($\mathcal{R}_1 = 0.458$ et $\mathcal{R}_2 = 0.0068$). In Figs. 5-7, we used: $\gamma_V = 3459 \times 10^6$, $b_{HD} = 43910$, $I_U(0) = 20$, $I_L(0) = 5$, $F(0) = 100$, $V_U(t) = 10$, $H_U(t) = 700$, $V_L(t) = 10$, $H_L(t) = 400$ for all $t \in [-\tau, 0]$ ($\mathcal{R}_1 = 4587.68$ et $\mathcal{R}_2 = 304.514$).

The Figs. 1-4 show the distribution of virus and infected cells in the URT and LRT respectively, completely destroyed over time. However, the latency period can cause several states of chronic infection before total recovery. We also observe that the density of viruses increases as the latent period is large. This could be due to the fact that the immune system is alerted with a delay, which works in favor of the replication of viruses.

Figs. 5-7 illustrate the distribution of healthy, infectious epithelial cells and virus respectively in the two respiratory tracts. The dashed and strong line curves represent the lower and upper airways, respectively. In Fig. 5, we observe a periodic behavior; the peak in the population of healthy cells is reached at the latency time.

5. Conclusion

In this work, we analyzed a virus model of SARS-Cov-2 infection with immune response. The initial model was formulated by Mochan et al. [23] to describe an experiment made on macaques. Unlike their model, we did not explicitly represent the classes of damage cellular caused by infection and death of cells, and anti-inflammatory mediators created directly in response to pro-inflammatory signals. However, we considered the latent period of newly infected cells by introducing a time-delay in the model. We fully studied the qualitative property of the model, investigated strategies

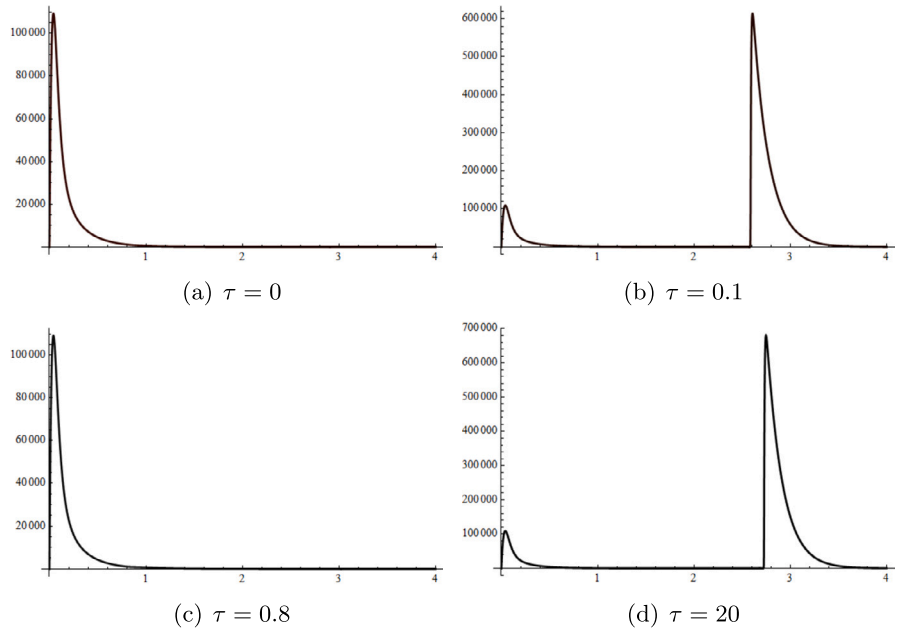

Fig. 1. Distribution of virus in the URT.

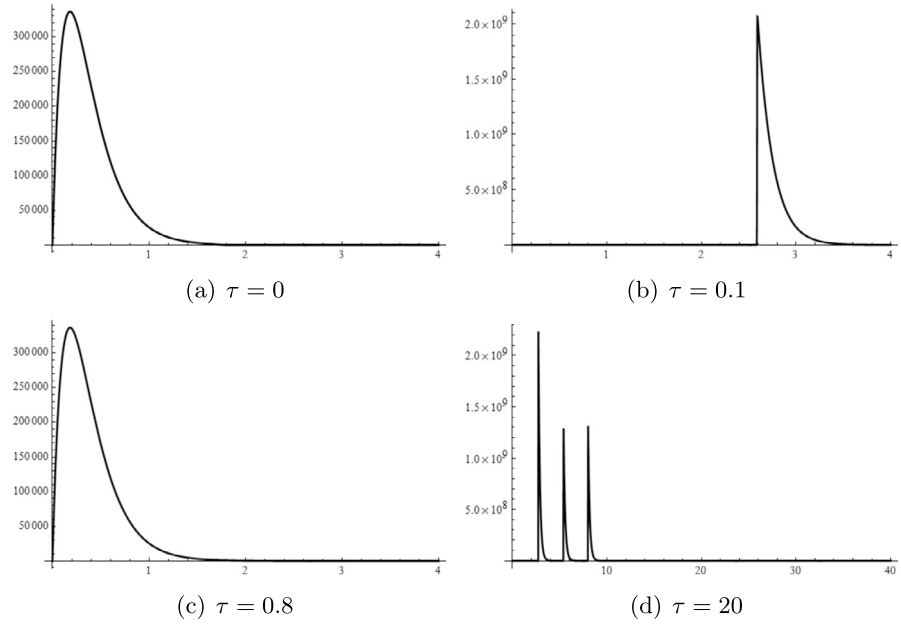

Fig. 2. Distribution of virus in the LRT.

to reduce cell infection, and assessed the effect of the latency period on the spread of the infections. We found out that epithelial cells cannot be completely cleared in a respiratory tract. We also observed the possibility to overcome infections and viruses when $\mathcal{R}_0 > 1$. This observation is not possible when the latent period is overlooked. Moreover, we established the occurrence of a Hopf bifurcation when $\mathcal{R}_0 > 1$. The sensitivity index analysis revealed that reducing the replication rate of viruses or increasing the depletion rate of cells are the best strategies to reduce secondary infections. We further investigated the optimal cost to implement these strategies. We established the existence of the optimal solution. In contrast to Mochan et al. [23] findings, our simulations show that increased suppression of virus growth can change a lethal or chronic infection to acute infection (see Fig. 1 and Fig. 7).

The analysis presented in this work is a quantitative tool to understand the dynamics of viral cell infection. It also highlights the importance of the latent period and the impact of drug therapy in lowering infections. Since the model we analyzed is by necessity a simplification of the complex interactions and dynamics in the immune response, future extensions of this work may include more components of the immune response. We will also consider derivatives of fractional order because they extend the classical derivatives used in this work and have been proven to capture more information (see [3,4,1,15]).

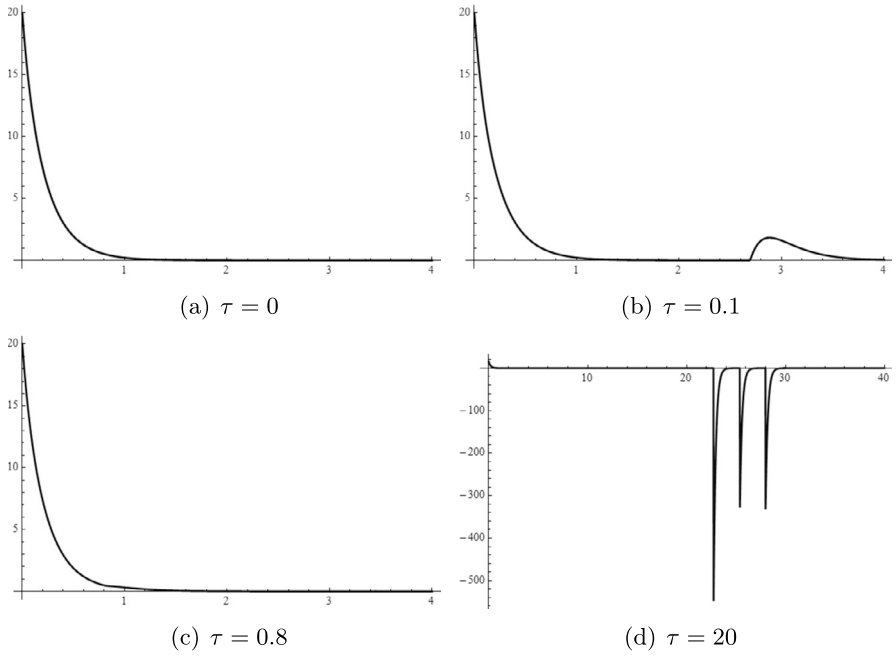

Fig. 3. Distribution of infected cells in the URT. We observe a negative solution when $\tau = 20$.

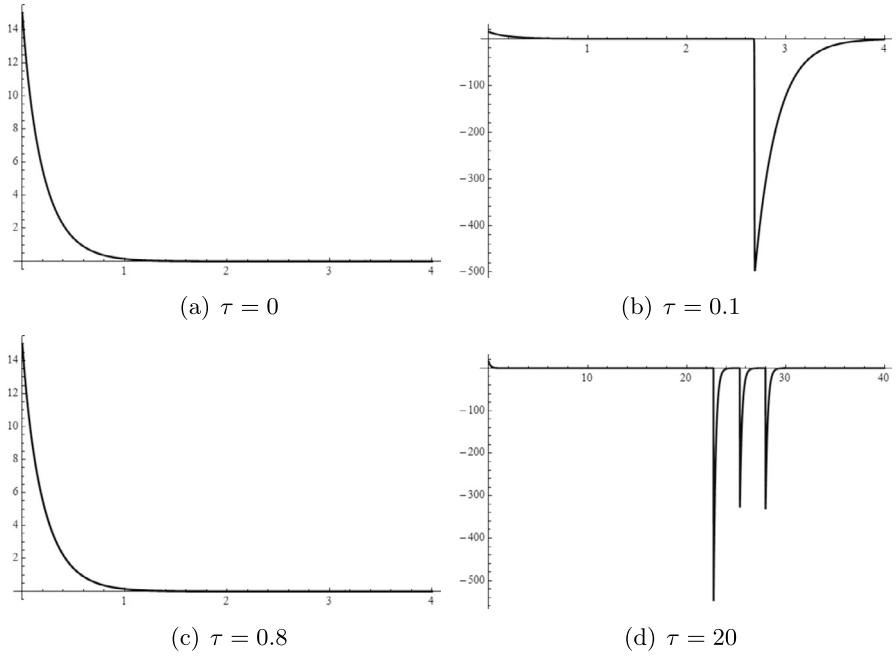

Fig. 4. Distribution of infected cells in the LRT. We observe that the latent period changes the sign of the solution.

Declaration of competing interest

The authors declare that they have no known competing financial interests or personal relationships that could have appeared to influence the work reported in this paper.

Acknowledgements

The support of the DST-NRF Centre of Excellence in Mathematical and Statistical Sciences (CoE-MaSS) towards this research is hereby acknowledged. Opinions expressed and conclusions arrived at are those of the authors and not necessarily to be attributed to the CoE-MaSS.

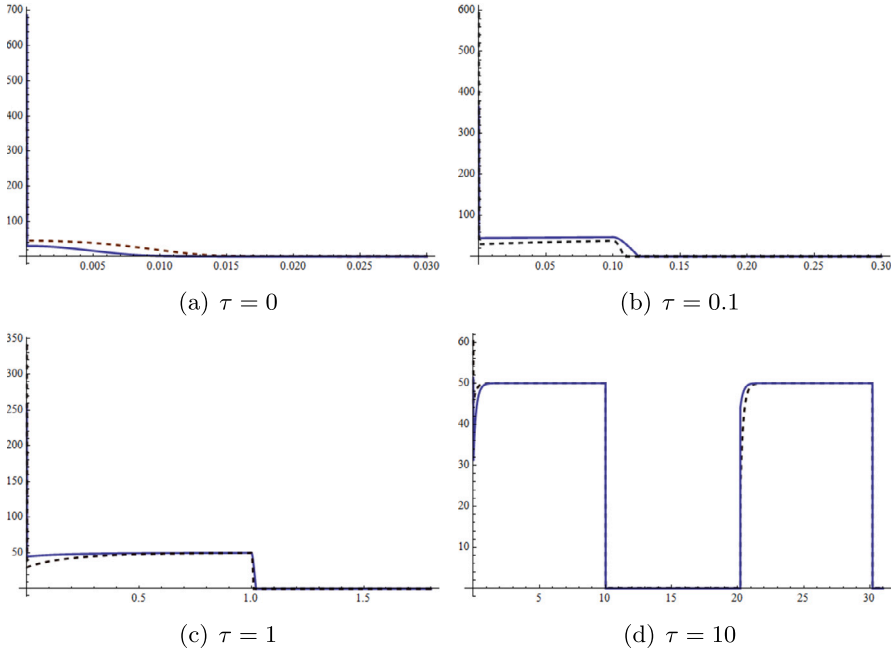

Fig. 5. Distribution of healthy cells in both respiratory tracts in an endemic infection scenario.

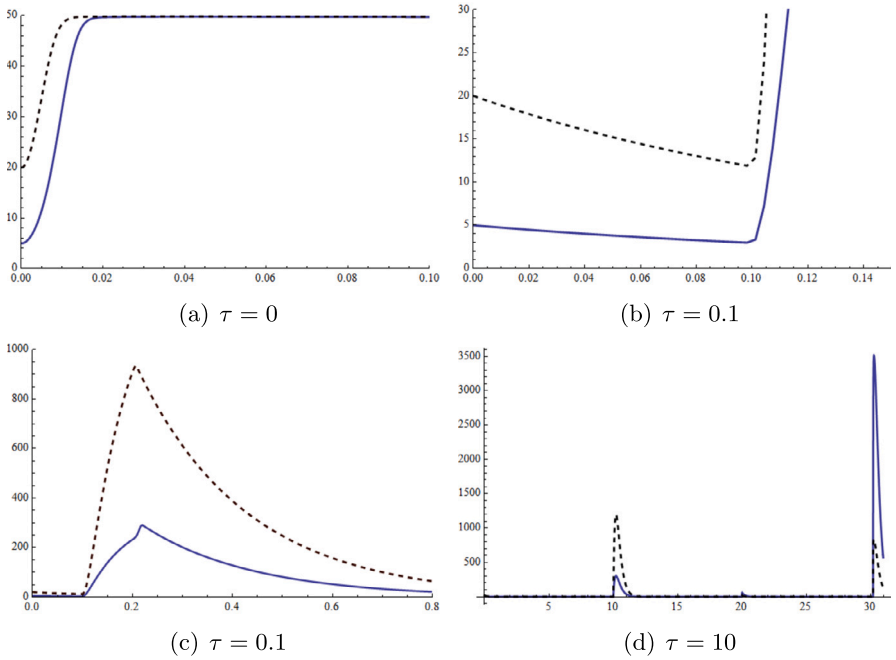

Fig. 6. Distribution of infected cells in both respiratory tracts in an endemic infection scenario.

References

[1] A. Alkhazzan, J. Wang, Y. Nie, H. Khan, J. Alzabut, A stochastic SIRS modeling of transport-related infection with three types of noises, Alex. Eng. J. 76 (2023) 557–572.
[2] A. Atangana, S. Araz, Mathematical model of COVID-19 spread in Turkey and South Africa: theory, methods, and applications, Adv. Differ. Equ. 2020 (2020) 659.
[3] D. Baleanu, S. Arshad, A. Jajarmi, W. Shokat, F. Akhavan Ghassabzade, M. Wali, Dynamical behaviours and stability analysis of a generalized fractional model with a real case study, J. Adv. Res. 48 (2023) 157–173.
[4] D. Baleanu, M. Hassan Abadi, A. Jajarmi, K. Zarghami Vahid, J.J. Nieto, A new comparative study on the general fractional model of COVID-19 with isolation and quarantine effects, Alex. Eng. J. 61 (2022) 4779–4791.
[5] Y. Cao, W. Gao, L. Caro, J.A. Stone, Immune-viral dynamics modeling for SARS-CoV-2 drug development, Clin. Transl. Sci. 14 (6) (2021) 2348–2359.
[6] J.F.W. Chan, S. Yuan, K.H. Kok, K.K.W. To, H. Chu, J. Yang, F. Xing, J. Liu, C.C.Y. Yip, R.W.S. Poon, et al., A familial cluster of pneumonia associated with the 2019 novel coronavirus indicating person-to-person transmission: a study of a family cluster, Lancet 395 (2020) 514–523.
[7] B. Chatterjee, H. Singh Sandhu, N.M. Dixit, Modeling recapitulates the heterogeneous outcomes of SARS-CoV-2 infection and quantifies the differences in the innate immune and CD8 T-cell responses between patients experiencing mild and severe symptoms, PLoS Pathog. 18 (6) (2022) e1010630.
[8] T. Chen, J. Rui, Q. Wang, et al., A mathematical model for simulating the phase-based transmissibility of a novel coronavirus, Infect. Dis. Poverty 9 (2020) 24.

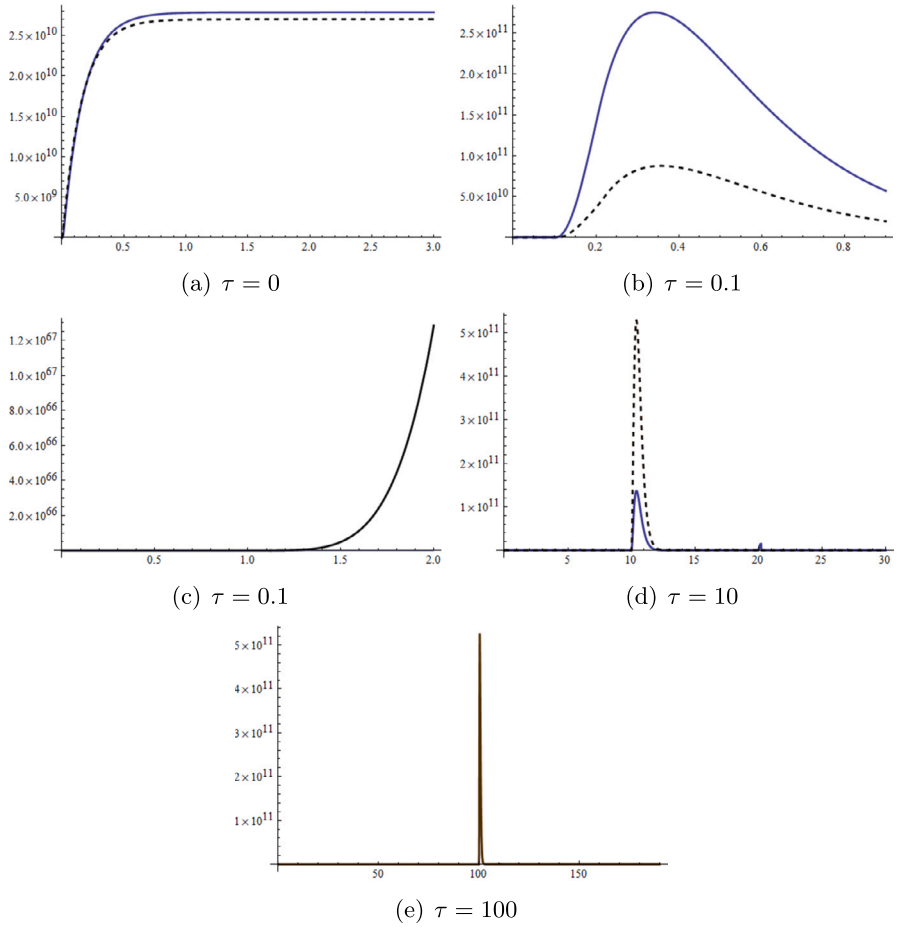

Fig. 7. Distribution of virus in both respiratory tracts in an endemic infection scenario.

[9] W. Fleming, R. Rishel, Deterministic and Stochastic Optimal Control, Springer-Verlag, New York, 1975.
[10] G. Giordano, F. Blanchini, R. Bruno, et al., Modelling the COVID-19 epidemic and implementation of population-wide interventions in Italy, Nat. Med. 26 (2020) 855–860.
[11] L. Göllmann, D. Kern, H. Maurer, Optimal control problems with delays in state and control and mixed control-state constraints, Optim. Control Appl. Methods 30 (4) (2008) 341–365.
[12] W.J. Guan, Z.Y. Ni, Y. Hu, W.H. Liang, C.Q. Ou, J.X. He, L. Liu, H. Shan, et al., Clinical characteristics of coronavirus disease 2019 in China, N. Engl. J. Med. 382 (2020) 1708–1720.
[13] C. Huang, Y. Wang, X. Li, L. Ren, J. Zhao, Y. Hu, L. Zhang, G. Fan, J. Xu, X. Gu, et al., Clinical features of patients infected with 2019 novel coronavirus in Wuhan, China, Lancet 395 (2020) 497–506.
[14] K.J. Huang, I.J. Su, M. Theron, Y.C. Wu, S.K. Lai, C.C. Liu, H.Y. Lei, An interferon-γ-related cytokine storm in SARS patients, J. Med. Virol. 75 (2005) 185–194.
[15] S. Hussain, O. Tunç, G. Rahman, H. Khan, E. Nadia, Mathematical analysis of stochastic epidemic model of MERS-corona & application of ergodic theory, Math. Comput. Simul. 207 (2023) 130–150.
[16] N. Imai, A. Cori, I. Dorigatti, M. Baguelin, C.A. Donnelly, S. Riley, N.M. Ferguson, Report 3: Transmissibility of 2019-nCoV, Imperial College London, London, UK, 2020.
[17] L. Jia, Z. Chen, Y. Zhang, L. Ma, L. Wang, X. Hu, H. Liu, J. Chen, D. Liu, W. Guan, Suppression and activation of intracellular immune response in initial severe acute respiratory syndrome coronavirus 2 infection, Front. Microbiol. 12 (2021) 768740, https://doi.org/10.3389/fmicb.2021.768740. PMID: 34899651; PMCID: PMC8661415.
[18] L. Josset, F. Engelmann, K. Haberthur, et al., Increased viral loads and exacerbated innate host responses in aged Macaques infected with the 2009 Pandemic H1N1 Influenza A virus, J. Virol. 86 (2012) 11115–11127.
[19] S.A. Lauer, K.H. Grantz, Q. Bi, F.K. Jones, Q. Zheng, H.R. Meredith, A.S. Azman, N.G. Reich, J. Lessler, The incubation period of coronavirus disease 2019 (COVID-19) from publicly reported confirmed cases: estimation and application, Ann. Intern. Med. 172 (2020) 577–582.
[20] Q. Li, X. Guan, P. Wu, X. Wang, L. Zhou, Y. Tong, R. Ren, K.S. Leung, et al., Early transmission dynamics in Wuhan, China, of novel coronavirus-infected pneumonia, N. Engl. J. Med. 382 (2020) 1199–1207.
[21] Z. Memon, S. Qureshi, B.R. Memon, Assessing the role of quarantine and isolation as control strategies for COVID-19 outbreak: a case study, Chaos Solitons Fractals 144 (2021) 110655.
[22] J.E. Mittler, et al., Influence of delayed viral production on viral dynamics in HIV-1 infected patients, Math. Biosci. 152 (1998) 143–163.
[23] E. Mochan, T. Sego, L. Gaona, E. Rial, G. Ermentrout, Compartmental model suggests importance of innate immune response to COVID-19 infection in rhesus macaques, Bull. Math. Biol. 83 (2021) 79.
[24] V.J. Munster, F. Feldmann, B.N. Williamson, et al., Respiratory disease in rhesus macaques inoculated with SARS-CoV-2, Nature 585 (2020) 268–272.
[25] S. Musa, Qureshi, S. Zhao, A. Yusuf, U. Mustapha, D. He, Mathematical modeling of COVID-19 epidemic with effect of awareness programs, Infect. Dis. Model. 6 (2021) 448–460.
[26] P.W. Nelson, J.D. Murray, A.S. Perelson, A model of HIV-1 pathogenesis that includes an intracellular delay, Math. Biosci. 163 (2000) 201–215.
[27] M.L. Ng, J.W. Lee, M.L. Leong, A.E. Ling, H.C. Tan, E.E. Ooi, Topographic changes in SARS coronavirus-infected cells at late stages of infection, Emerg. Infect. Dis. 10 (11) (2004) 1907–1914, https://doi.org/10.3201/eid1011.040195. PMID: 15550199; PMCID: PMC3328989.
[28] N. Parolini, L. Dede, P.F. Antonietti, et al., SUIHTER: a new mathematical model for COVID-19. Application to the analysis of the second epidemic outbreak in Italy, Proc. R. Soc. A 477 (2021) 20210027.
[29] R. Pung, C.J. Chiew, B.E. Young, S. Chin, M.I. Chen, H.E. Clapham, A.R. Cook, et al., Investigation of three clusters of COVID-19 in Singapore: implications for surveillance and response measures, Lancet 395 (2020) 1039–1046.
[30] J.M. Read, J.R.E. Bridgen, D.A.T. Cummings, A. Ho, C.P. Jewell, Novel coronavirus 2019-nCoV (COVID-19): early estimation of epidemiological parameters and epidemic size estimates, Philos. Trans. R. Soc. Lond. B, Biol. Sci. 376 (1829) (2021) 20200265.
[31] M.Z. Tay, C.M. Poh, L. Rénia, P.A. MacAry, L.F. Ng, The trinity of COVID-19: immunity, inflammation and intervention, Nat. Rev. Immunol. 20 (2020) 363–374.

[32] B. Tang, X. Wang, Q. Li, N.L. Bragazzi, S. Tang, Y. Xiao, J. Wu, Estimation of the transmission risk of the 2019-nCoV and its implication for public health interventions, J. Clin. Med. 9 (2020) 462.
[33] P.M. Tchepmo Djomegni, M.S. Daoussa Haggar, W. Tiruneh Adigo, Mathematical model for Covid-19 with protected susceptible in the post-lockdown era, Alex. Eng. J. 60 (1) (2011) 527–535.
[34] S. Wang, Y. Pan, Q. Wang, H. Miao, A.N. Brown, L. Rong, Modeling the viral dynamics of SARS-CoV-2 infection, Math. Biosci. 328 (2020) 108438.
[35] J.T. Wu, K. Leung, G.M. Leung, Nowcasting and forecasting the potential domestic and international spread of the 2019-nCoV outbreak originating in Wuhan, China: a modelling study, Lancet 395 (2020) 689–697.
[36] C. Yang, J. Wang, A mathematical model for the novel coronavirus epidemic in Wuhan, China, Math. Biosci. Eng. 17 (2020) 2708–2724.